



FINAL REPORT

MAGNETIC NANOPARTICLES COATED WITH ZWITTERIONIC COPOLYMER FOR LABEL-FREE COLORIMETRIC DETECTION OF PATHOGENIC BACTERIA

BY

DR. PIYAPORN NA NONGKHAI PROF. DR. VORAVEE P. HOVEN

THIS PROJECT GRANTED BY THE THAILAND

RESEARCH FUND

MAY/2020

Final Report

Magnetite nanoparticles coated with zwitterionic copolymer for label-free colorimetric detection of pathogenic bacteria

Researcher	Institute
Dr. Piyaporn Na Nongkhai	Department of Chemistry, Faculty of Science,
	Burapha University
Prof. Dr. Voravee P. Hoven	Department of Chemistry, Faculty of Science,
	Chulalongkorn University

This project granted by Office of the Higher Education and the Thailand Research Fund

ABSTRACT

Magnetite nanoparticles (Fe₃O₄ NPs) are recognized as potential nanomaterials for biosensing applications which are mostly relied on their magnetic property for separating and capturing the target analyte. Their enzyme-mimic catalytic property also provides an additional feature that can be used for signal amplification in colorimetric detection. Here in this research, a simple colorimetric assay for biomolecule detection based on target-induced shielding effect using Fe₃O₄ NPs coated with zwitterionic copolymer in combination with label-free aptamers was developed. Zwitterionic copolymer of poly[(methacrylic acid)-co-(2-methacryloyloxyethyl phosphorylcholine)] (PMAMPC) is particularly chosen not only to provide active carboxyl groups for anchoring the aptamers, but also to inherit anti-fouling characteristic to the Fe₃O₄ NPs so that adsorption of non-targeted analyte and contaminants may be suppressed once subjected to real sample analysis. Vibrio parahaemolyticus (V. parahaemolyticus), foodborne pathogenic bacteria found in seafood was used as model for evaluating the biosensing activity of the developed Fe₃O₄ NPs. In the presence of target bacteria, the catalytic activity of Fe₃O₄ NPs would be inhibited resulting in the decrease of color change which could be realized by naked eye and quantified by spectrophotometer. As opposed to the conventional assays based on ELISA or PCR technology, this one-step assay should definitely be more rapid and economical and easily implemented for field and on-site screening tests.

Keywords (3-5 words): magnetite nanoparticles, biosensor, colorimetric detection, pathogenic bacteria

Project Code: MRG6180133

Project Title: Magnetite nanoparticles coated with zwitterionic copolymer for label-free colorimetric

detection of pathogenic bacteria

Investigator: Dr. Piyaporn Na Nongkhai

E-mail Address: piyapornn@buu.ac.th

Project Period: 2 Years

Abstract: Magnetite nanoparticles (Fe₃O₄ NPs) are recognized as potential nanomaterials for biosensing applications which are mostly relied on their magnetic property for separating and capturing the target analyte. Their enzyme-mimic catalytic property also provides an additional feature that can be used for signal amplification in colorimetric detection. Here in this research, a simple colorimetric assay for biomolecule detection based on target-induced shielding effect using Fe₃O₄ NPs coated with zwitterionic copolymer in combination with label-free aptamers was of poly[(methacrylic developed. Zwitterionic copolymer acid)-co-(2-methacryloyloxyethyl phosphorylcholine)] (PMAMPC) is particularly chosen not only to provide active carboxyl groups for anchoring the aptamers, but also to inherit anti-fouling characteristic to the Fe₃O₄ NPs so that adsorption of non-targeted analyte and contaminants may be suppressed once subjected to real sample analysis. Vibrio parahaemolyticus (V. parahaemolyticus), foodborne pathogenic bacteria found in seafood was used as model for evaluating the biosensing activity of the developed Fe₃O₄ NPs. In the presence of target bacteria, the catalytic activity of Fe₃O₄ NPs would be inhibited resulting in the decrease of color change which could be realized by naked eye and quantified by spectrophotometer. As opposed to the conventional assays based on ELISA or PCR technology, this one-step assay should definitely be more rapid and economical and easily implemented for field and on-site screening tests.

Keywords (3-5 words): magnetite nanoparticles, biosensor, colorimetric detection, pathogenic bacteria

TABLE OF CONTENTS

ACKNOWLEDGEMENTS	1
OUTPUT	2
ABSTRACT	8
EXCUTIVE SUMMARY	3
OBJECTIVE	4
1. INTRODUCTION	5
2. RESEARCH METHODOLOGY	7
2.1 Preparation and characterization of polymer-coated Fe ₃ O ₄ NPs	7
2.2 Immobilization of sensing probe	8
2.3 Investigation of peroxidase catalytic activity	9
2.4 Examination of colorimetric assay for bacteria detection	10
2.4.1 Bacterial culture	10
2.4.2 Detection of <i>V. parahaemolyticus</i>	10
2.4.3 Detection of <i>V. parahaemolyticus</i> in spiked oyster samples	10
3. RESULT AND DISCUSSION	12
3.1 Preparation and characterization of polymer-coated Fe ₃ O ₄ NPs	12
3.2 Immobilization of sensing probe	14
3.3 Investigation of peroxidase catalytic activity	16
3.4 Examination of colorimetric assay for bacteria detection	18
3.4.1 Detection of V. parahaemolyticus in the pure cultures	21
3.4.2 Detection of <i>V. parahaemolyticus</i> in spiked samples	23
4. CONCLUSION	25
5. REFERENCE	26

TABLE OF FIGURES

Figure 1. Schematic method for preparation Fe ₃ O ₄ NPs coated with PMAMPC	7
Figure 2. Schematic method for sensing probe Immobilization	9
Figure 3. Peroxidase catalytic activity of aptamer-conjugated Fe ₃ O ₄ NPs-PMAMPC	9
Figure 4. Schematic method for bacteria detection by aptamer-conjugated Fe ₃ O ₄ NPs-	
PMAMPC	11
Figure 5. ATR-FTIR of uncoated Fe ₃ O ₄ NPs and Fe ₃ O ₄ NPs-PMAMPC	12
Figure 6. TGA curves of (a) uncoated Fe ₃ O ₄ NPs and (b) PMAMPC-Fe ₃ O ₄ NPs	13
Figure 7. Pictures of uncoated Fe ₃ O ₄ NPs PMAMPC-Fe ₃ O ₄ NPs colloidal suspensions after	
30-day of storage without an external field	14
Figure 8. Pictures of PMAMPC-Fe ₃ O ₄ NPs colloidal after exposure to an external magnetic	14
field (left) and magnetization curves of PMAMPC-Fe ₃ O ₄ NPs (right)	
Figure 9. ATR-FTIR spectrum of uncoated Fe ₃ O ₄ NPs (a), Fe ₃ O ₄ NPs-PMAMPC (b), Apt-MNPs@12.5	15
μL (c), Apt-MNPs@25 μL (d) and Apt-MNPs@50 μL (e)	
Figure 10. Fluorescence spectra of initial FAM-labelled complementary DNA (a), remaining FAM-	16
labelled complementary DNA@12.5 µM apt (b), remaining FAM-labelled complementary	
DNA@25 μM apt, and remaining FAM-labelled complementary DNA@50 μM apt	
Figure 11. The catalytic activity of uncoated Fe_3O_4NPs , Fe_3O_4NPs -PMAMPC and Apt-MNPs	17
Figure 12. The catalytic activity of Apt-MNPs at different amount of aptamer immobilization	17
Figure 13. Schematic representation of colorimetric of a foodborne pathogen by aptamer-conjugated	
Fe ₃ O ₄ NPs	18
Figure 14. Schematic representation of colorimetric detection of <i>V. parahaemolyticus</i> by aptamer-	
conjugated Fe₃O₄NPs	19
Figure 15. Optimization of the nanoparticles amount (A) and the conjugated aptamer amount (B).	
The concentration of <i>V. parahaemolyticus</i> was 10 ⁴ cfu/mL	20
Figure 16. Optimization of $\mathrm{H_2O_2}$ concentration (A) and TMB concentration (B) The concentration of	
<i>V. parahaemolyticu</i> s was 10⁴ cfu/mL	21
Figure 17. (A) Optical images and (B) absorption spectra form the detection of different	
concentrations of V. parahaemolyticus (C) Standard curve of the related absorbance	
versus the log concentration of <i>V. parahaemolyticus</i>	22
Figure 18. (A) Absorption spectra and relevance optical images form the detection of different	
concentrations of V. parahaemolyticus in spiked samples (B) Standard curve of the	
related absorbance versus the log concentration of V. parahaemolyticus	23
Figure 19. Specificity evaluation against other bacteria. Concentration of bacteria was 10 ⁴ cfu/mL	24

ACKNOWLEDGEMENTS

First of all, this project would have not been possible without the support by the Thailand Research Fund (Contract No. MRG6180133) for providing seed money for this project. I also would like to thank my mentor, Prof. Dr. Voravee P. Hoven for her valuable guidance and proof reading of the manuscript. I also would like to thank my students, Miss Supannika Boonjamnian and Miss Varunee Sadsri for their hard works carrying out the experiments, writing the first draft of the manuscripts and analyzing the data. Finally, I would like to thank the Department of Chemistry, Faculty of Science, Burapha University for all facilities and supports

Piyaporn Na Nongkhai May/2020

OUTPUT

1. International publication

Varunee Sadsri, Thanida Trakulsujaritchok, Marut Tangwattanachuleeporn, Voravee P. Hoven, and Piyaporn Na Nongkhai. A simple colorimetric assay for Vibrio parahaemolyticus detection using aptamer-functionalized nanoparticles. ACS Omega (2020) **Under Revision.**

2. Conferences

Varunee Sadsri and Piyaporn Na Nongkhai. (2019) The application of aptamer-immobilized PMAMPC-Fe₃O₄NPs for pathogenic bacteria detection. The international polymer conference of Thailand (PCT-9) 2019, Bangkok, Thailand, June 13-14, 2019.

EXECUTIVE SUMMARY

The research title of magnetite nanoparticles coated with zwitterionic copolymer for label-free colorimetric detection of pathogenic bacteria aims to develop a simple colorimetric biosensor employing Fe₃O₄ NPs coated with zwitterionic copolymer and conjugated with label-free aptamers for bacteria detection. The detection is simple and can be estimated by naked eye and more accurately monitored by spectrophotometer. It should be highlighted that this assay does not require additional step for signal amplification as traditional assay. Moreover, as opposed to the conventional assays based on ELISA or PCR technology, this one-step assay should definitely be more rapid and economical and easily implemented for field and on-site screening tests. The outputs of this project are one international publication and one presentation in the international conference.

OBJECTIVE

To develop a simple colorimetric assay for pathogenic bacteria detection based on ${\rm Fe_3O_4}$ NPs coated with zwitterionic copolymer.

1. INTRODUCTION

At present, iron oxide nanoparticles (IONPs), especially magnetite nanoparticles (Fe₃O₄ NPs), have been subjected to extensive research due to their potential applications in the fields of biotechnology and biomedicine. Especially, Fe₃O₄ NPs have gained an increasing attention in the development and applications of biosensors. In general, Fe₃O₄ NPs are used to separate and capture the target biomolecules and then signal can be detected using additional amplification methods such as real-time polymerase chain reaction (PCR) (Yang *et al.*, 2007; Mao *et al.*, 2016), fluorescence (Zeng *et al.*, 2014; Wan *et al.*, 2014; Shukla *et al.*, 2016), magnetic relaxation switching (Chen *et al.*, 2015) as well as enzyme-linked immunosorbent assay (ELISA) (Gao *et al.*, 2007; Zhang *et al.*, 2010; Woo *et al.*, 2013) which need expensive instruments and highly skilled operators. Interestingly, it has been discovered by Gao and co-worker (Gao *et al.*, 2007) that Fe₃O₄ NPs exhibit intrinsic enzyme-mimic activity similar to natural peroxidase enzymes, such as horseradish peroxidase (HRP), a common labeling reagent in ELISA. Therefore, Fe₃O₄ NPs can be employed in colorimetric-based biosensor of which signal amplification relying on the ability of Fe₃O₄ NPs to catalyze the oxidation of organic substrate to produce a color change that can be monitored by an instrument or naked eye. In principle, the size as well as surface functionality of Fe₃O₄ NPs largely affects their catalytic activity which can be tuned by methodologies selected for synthesis and chemical modification

Practical surface functionalization should not only provide nanoparticles with good colloidal stability under usual conditions such as 0.9% NaCl and PBS but also offers as many functional groups as possible so that efficient conjugation of sensing probe such as protein, antibody, DNA and aptamer can be achieved. The active functional groups on the surface such as carboxylates, amines, or thiols, provide a strong linkage between the iron oxide and sensing probe. Among several surface functionalization methods, polymer coating has been widely used to stabilize Fe₃O₄ NPs by providing electrostatic and steric repulsion against particle aggregation. Moreover, multiple functional groups along polymer chains also serve as active sites for further functionalization (Mahmoudi *et al.*, 2011, Jiang *et al.*, 2012, Xu *et al.*, 2013). A simple and versatile method for coating the polymer onto the Fe₃O₄ NPs' surface is based on the chemical interaction between iron atom and ligand, so-called chelation, which can be achieved either via the *in situ* coatings during nanoparticles synthesis or the post-synthesis coatings after nanoparticles formation. Carboxylate ions of carboxylic acid-containing polymer such as poly(acrylic acid) show high affinity towards iron atom on the Fe₃O₄ NPs' surface via coordination (Chui *et al.*, 2008, Cirtiu *et al.*, 2011, Wang *et al.*, 2014) thus providing high stability in aqueous media and enough free carboxylic acid groups for further sensing probe conjugation.

The ability to specifically interact with target molecules as opposed to the non-targeted components is another important issue to be taken into consideration when developing a biosensing platform to be used for analysis of real samples having numerous types of non-related components. The nonspecific adsorption usually leads to high background noise or a low signal-to-noise ratio (S/N) which significantly affects the selectivity and sensitivity of the sensor. Poly(2-methacryloyloxyethyl phosphorylcholine) (PMPC), has been recently recognized as an hydrophilic zwitterionic polymer that can effectively reduce nonspecific adsorption of proteins (Park *et al.*, 2007; Tajima *et al.*, 2011; Nishizawa *et al.*, 2011). In our previous work, novel PMPC-based copolymer, namely poly[(methacrylic acid)-*co*-(2-methacryloyloxyethyl phosphorylcholine)] (PMAMPC), also showed the success of MPC units in suppressing nonspecific protein adsorption on gold surface of an SPR sensor chip (Akkahat *et al.*, 2012). The carboxyl groups from the MA units of PMAMPC were also useful for attaching active biomolecules that

can act as sensing probes for biospecific detection of targeted molecules. From the dual functionality of PMAMPC, PMAMPC-based SPR sensor provided a high detection efficiency of the targeted molecules in diluted blood plasma samples. For these reasons, PMAMPC can be a potential candidate for Fe₃O₄ NPs modification. Although Fe₃O₄ NPs have been applied for colorimetric biosensors, most of detection assays rely on conventional ELISA which requires another capture probe coating onto an ELISA plate for signal amplification (Gao *et al.*, 2007; Zhang *et al.*, 2010; Woo *et al.*, 2013). Moreover, nonspecific adsorption of non-targeted molecules has also been observed.

Therefore, this research aims to develop a simple colorimetric biosensor employing Fe₃O₄ NPs coated with PMAMPC and conjugated with label-free aptamers (aptamer-conjugated Fe₃O₄ NPs-PMAMPC)) for bacteria detection. First, Fe₃O₄ NPs-PMAMPC are synthesized by "one-pot reaction" based on a combination of chemical co-precipitation and chelation. Given that carboxylate ions in PMAMPC being capable of chelating with Fe₃O₄ NPs (Chui et al., 2008, Cirtiu et al., 2011, Wang et al., 2014), PMAMPC coating can be done in situ during the formation of Fe₃O₄ NPs by co-precipitation. In addition, the free carboxyl groups of PMAMPC can also conjugate with nucleic acid aptamers that specifically capture target bacteria. Vibrio parahaemolyticus (V. parahaemolyticus), foodborne pathogenic bacteria found in seafood is selected as model for evaluating the biosensing activity of the developed Fe₃O₄ NPs. One-step detection mechanism is designed based on the concept of target-induced shielding effect whereby the catalytic activity of aptamer-conjugated Fe₃O₄ NPs-PMAMPC would be suppressed in the presence of bacteria (Figure 1). In principle, the extent of inhibition should be varied as a function of bacteria concentration so that the bacterial quantification can be estimated by naked eye and more accurately monitored by spectrophotometer. It should be highlighted that this assay does not require additional step for signal amplification as traditional assay. Moreover, from the ability to suppress the nonspecific adsorption of MPC groups in the coated zwitterionic copolymer, our biosensor should provide a high sensitivity and selectivity. The fundamental knowledge gained from this research should be highly beneficial for the development of label-free, low-cost, and simple biosensors.

2. RESEARCH METHODOLOGY

2.1 Preparation and characterization of polymer-coated Fe₃O₄ NPs

Fe₃O₄NPs were prepared and coated with PMAMPC using two-step in situ methods. The Fe₃O₄NPs were firstly formed by chemical co-precipitation of ferrous/ferric ions in alkaline medium and then PMAMPC solution was directly added to Fe₃O₄NPs suspension providing a coating of PMAMPC on Fe₃O₄NPs through chelating bond. Typically, FeCl₃·6H₂O (298 mg, 1.10 mmol) and FeCl₂·4H₂O (109 mg, 0.55 mmol) were dissolved in 20 mL DI water at room temperature. After the salt was completely dissolved, the mixture was added to a flask under nitrogen atmosphere at 60 °C and mechanically stirred at 750 rpm for 30 min. 6 mL of aqueous ammonia solution (28%w/v) was slowly added and the solution color changed from orange to black. The colloidal mixture was continuously stirred for another hour. Subsequently, 40 mg of PMAMPC (PMA₃₇MPC₆₃, 54.5 kDa) corresponding to 68.8 μmol of carboxyl groups (COOH) was directly added to the black colloidal mixture. The mixture was stirred for 1 h and cooled to room temperature. The PMAMPC-Fe₃O₄NPs obtained were separated by a magnet and washed with DI water several times to remove unreacted chemicals. The PMAMPC- Fe₃O₄NPs were dispersed in distilled water and stored as aqueous colloidal suspensions.

The polymer-coated Fe_3O_4 NPs will be characterized by various analytical techniques. Their chemical functional, size and morphology will be characterized by attenuated total reflectance-Fourier transform- infrared spectroscopy (ATR FT-IR), transmission electron microscopy (TEM), respectively. The crystallization phase and magnetic properties will be studied by x-ray diffraction (XRD) and vibrating sample magnetometer (VSM), respectively. The amount of polymer coated on the Fe_3O_4 NPs will be evaluated by thermogravimetric analysis (TGA).

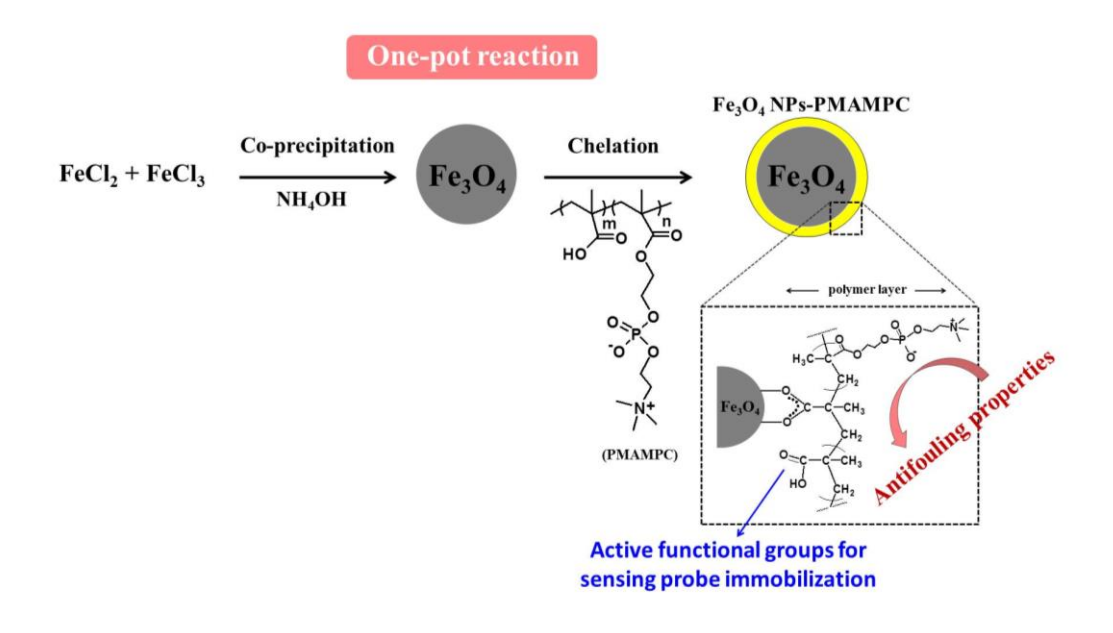


Figure 1 Schematic method for preparation Fe_3O_4 NPs coated with PMAMPC.

2.2 Immobilization of sensing probe

Amino-modified aptamer (NH₂-aptamer: 5'-NH₂-TCTAAAAATGGGCAAAGAACAGTGACTCGTTGAGAT ACT-3') will be used as *V. parahaemolyticus* sensing probe. The immobilization of sensing probe (NH₂-aptamer) will be done via amide bond formation between the amino group of NH₂-aptamer and the carboxyl group of the MA unit in the PMAMPC coated on the surface of Fe₃O₄ NPs. The carboxyl groups of the coated PMAMPC were first activated by an aqueous solution of EDC and NHS. Briefly, 250 μL of Fe₃O₄NPs-PMAMPC colloidal solution (10 mg/mL) was added to a fresh mixture of EDC (50 mg/mL, 50 μL) and NHS (50 mg/mL, 50 μL). The solution was incubated at room temperature with gentle shaking for 30 min, followed by magnetic separation. The resultant MNPs were dispersed in 50 μL of DI water and 50 μL of NH₂-aptamer (100 μM) was added and incubated for 45 min at room temperature with gentle shaking. Next, the aptamer-conjugated-Fe₃O₄NPs-PMAMPC were magnetically collected, rinsed with DI water and suspended in 500 μL of DI water to obtain the concentration of 5 mg/mL. The effects of NH₂-aptamer concentration on the immobilization efficiency will be investigated by changing the volume of NH₂-aptamer (100 μM) from 50 μL to 25 μL and 12.5 μL, respectively.

The amount of immobilized NH₂-aptamer was evaluated with fluorescence-labelled complementary DNA (5'-/56-FAM/AGT ATC TCA ACG AGT-3'). In experiment, 20 μ L of the aptamer-conjugated-Fe₃O₄NPs-PMAMPC (5 mg/mL) was dispersed in 70 μ L of DI water and 10 μ L of 100 μ M FAM-labelled complementary DNA was added into the solution. The reaction was continued for 45 min at room temperature with gentle shaking and then separated from the solution by a magnet. The supernatant was collected and determined the remaining FAM-labelled complementary DNA by fluorescence spectrophotometer. The amount of immobilized NH₂-aptamer on the PMAMPC-Fe₃O₄NPs surface was calculated in term of q_e using equations below.

$$q_e = (C_0 - C_e)V/m$$
 (1)

when q_e is the amount of immobilized NH₂-aptamer (mg/g)

C₀ is the initial concentration of FAM-labelled complementary DNA (mg/mL)

C_e is the remaining concentration of FAM-labelled complementary DNA (mg/mL)

V is the volume of the aqueous phase (mL)

m is the weight of the particles (g)

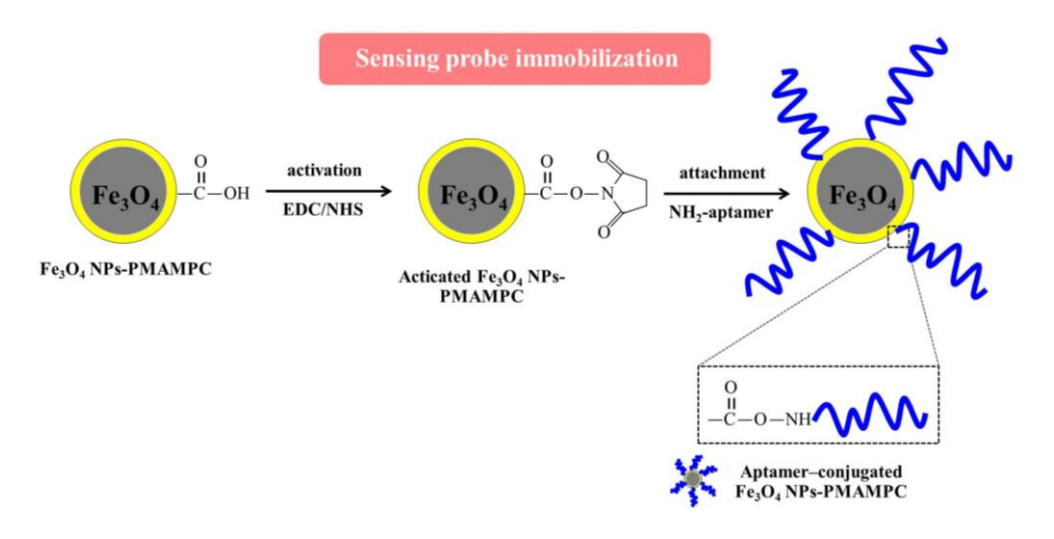


Figure 2 Schematic method for sensing probe Immobilization.

2.3 Investigation of peroxidase catalytic activity

The peroxidase catalytic activity of the aptamer-conjugated Fe_3O_4 NPs-PMAMPC will be examined by the oxidation reaction of 3,3',5,5'-tetramethylbenzidine (TMB) in a presence of H_2O_2 . Using UV-visible spectrophotometer, the peroxidase catalytic activity will be measured by monitoring a blue color of oxidized TMB of which intensity is directly proportional to catalytic activity. The effect of catalytic reaction time, pH solution and amount of the aptamer-conjugated Fe_3O_4 NPs-PMAMPC was investigated.

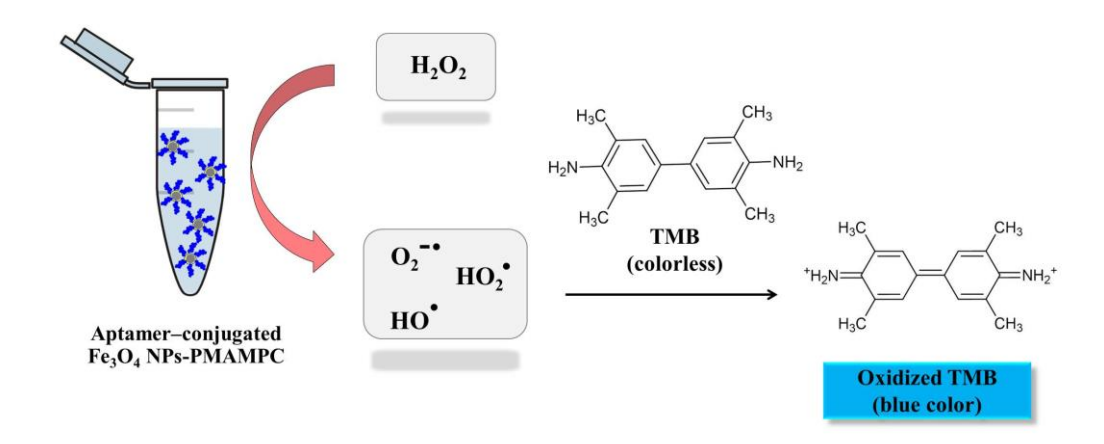


Figure 3 Peroxidase catalytic activity of aptamer-conjugated Fe₃O₄ NPs-PMAMPC

2.4 Examination of colorimetric assay for bacteria detection

In the final part, the applicability of aptamer-conjugated Fe_3O_4 NPs-PMAMPC for V. parahaemolyticus detection was examined. A simple colorimetric assay was carried out in one-step detection using TMB as substrate. The difference of color intensity between without and with V. parahaemolyticus was screened by naked eyes and quantified by spectrophotometer (Figure 4).

2.4.1 Bacterial culture.

The *V. parahaemolyticus* (ATCC 17802) was cultured overnight at 37 $^{\circ}$ C in alkaline peptone water (APW) with 1% NaCl (w/v) untill past the logarithmic phase. The culture was then diluted with a binding buffer (50 mM Tris-HCl at pH 7.4, 5 mM KCl, 100 mM NaCl, and 1 mM MgCl₂) until the OD_{600nm} = 0.5 (\sim 10 8 cfu/mL). The bacteria culture was then serially diluted 10-fold from 10 6 to 10 CFU/mL with binding buffer. Plate-counting was performed to verify the number of bacteria. One hundred μ L of the bacteria culture were diluted with selective medium and coated on agar plates (TCBS agar) and cultured at 37 $^{\circ}$ C for 18 hours to count colony-forming units (cfu).

2.4.2 Detection of V. parahaemolyticus

In the experiment, the cultured bacteria samples (1 mL) were centrifuged at 6000 rpm for 10 min and then 990 μ L of supernatant was removed. The bacteria pellet was diluted with 90 μ L of binding buffer. Then, 5 μ L of aptamer-conjugated Fe₃O₄ NPs-PMAMPC (1 mg/mL) was added to bacteria samples and incubated for 15 min at room temperature with gentle shaking. After that, 100 μ L of sodium acetate buffer (0.1 M, pH 3.6) , 20 μ L of TMB (1 mg/mL) and 20 μ L of H₂O₂ (0.1 M) was added and incubated at room temperature for 30 min. The absorption spectrum of the solution was measured with a UV-vis spectrophotometer.

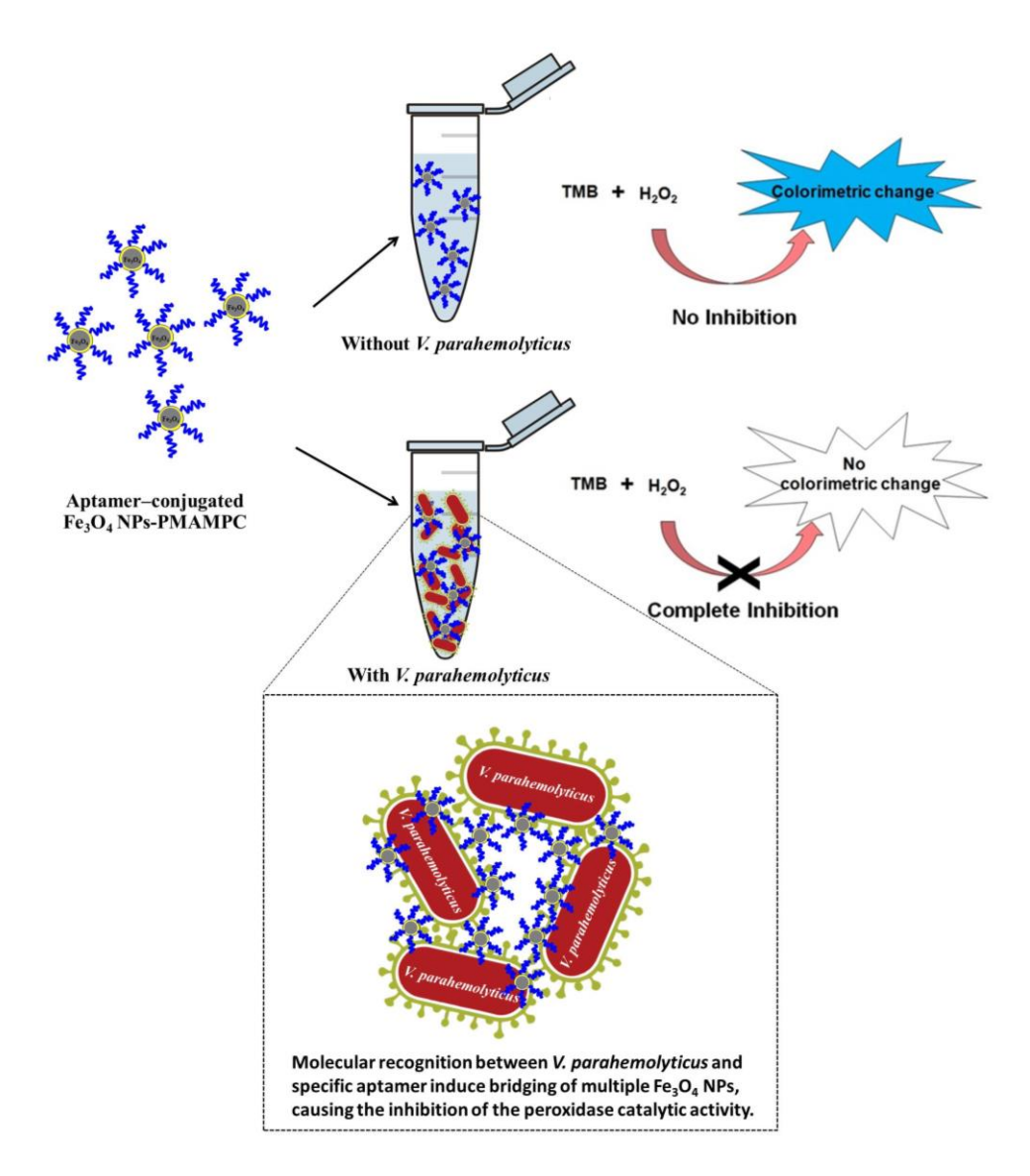
2.4.3 Detection of V. parahaemolyticus in spiked oyster samples

Oyster samples were purchased from a local market in Chonburi, Thailand, and 25 g of the oyster sample was immersed in 225 mL of binding buffer, followed by homogenization for 5 min. To prepare the spiked samples, the different concentrations of *V. parahaemolyticus* were added to the oyster sample. 1 mL of spiked samples was collected and centrifuged at 3000 rpm for 5 min to remove suspended particulate matter. Clear supernatant fluid was separated and subsequently filtered through a 0.45 µm membrane. Membrane filtration (MF) was used to separate and concentrate *V. parahaemolyticus* in samples fluid. After the filtration, the membrane was removed from the filtration apparatus and washed with 1 ml of binding buffer. The trapped *V. parahaemolyticus* was eluted from the membrane filter. The supernatant was transferred to a centrifuge tube and processed as described above.

The selectivity and sensitivity of this assay was also investigated. For specificity test, aptamer-conjugated Fe₃O₄ NPs–PMAMPC was used to detect other non-target bacteria such as *Escherichia coli (E. coli*). To quantify the sensitivity of this assay, linear relationship between bacterial concentrations and color intensity was monitored. The limit of detection (LOD) was calculated using equations below.

LOD = 3SDblank /m

when SD blank is standard deviation of absorbance in the absence *V. parahaemolyticus* m is slope of linear calibration curve of *V. parahaemolyticus*



 $\textbf{Figure 4} \ \, \textbf{Schematic method for bacteria detection by a ptamer-conjugated} \ \, \textbf{Fe}_{3}\textbf{O}_{4} \ \, \textbf{NPs-PMAMPC}$

3. RESULT AND DISCUSSION

3.1 Preparation and characterization of polymer-coated Fe₃O₄ NPs

ATR-FTIR analysis can be used to confirm the success of PMAMPC anchoring on the Fe $_3$ O $_4$ NPs surface. As demonstrated in Figure 5, a strong peak appearing at 580 cm $^{-1}$ corresponded to the characteristic band of Fe-O stretching vibration mode of Fe $_3$ O $_4$ NPs. The peaks at 1630 cm $^{-1}$ could be assigned to the stretching vibration of the hydroxyl group on the surface of the Fe $_3$ O $_4$ NPs. The characteristic bands of PMAMPC showed C=O, P-O and N $^+$ (CH $_3$) $_3$ stretching vibration at 1710, 1094 and 975 cm $^{-1}$, respectively. The presence of the chelating bond was observed at 1589 cm $^{-1}$ and 1412 cm $^{-1}$ which can be assigned to the asymmetric and symmetric C-O stretching modes of carboxylate groups. Moreover, the wavenumber separation (Δ), between the asymmetric and symmetric C-O stretching of carboxylate bands can be used to distinguish the coordination types, i.e. monodentate, bidentate and bridging complexes. The large Δ (>200 cm $^{-1}$) corresponds to the monodentate interaction and the small Δ (<110 cm $^{-1}$) is the bidentate interaction. The medium range Δ (140-200 cm $^{-1}$) was the bridging interaction. In this work, the Δ value is 177 cm $^{-1}$ (1589-1412 = 177 cm $^{-1}$) indicating that two Fe atoms chelated with two carboxylate oxygens, agreeing with the reported bonding between poly(acrylic acid) and Fe $_3$ O $_4$ NPs. From the above observations, we can confirm that PMAMPC was chemically anchored on the surface of Fe $_3$ O $_4$ NPs.

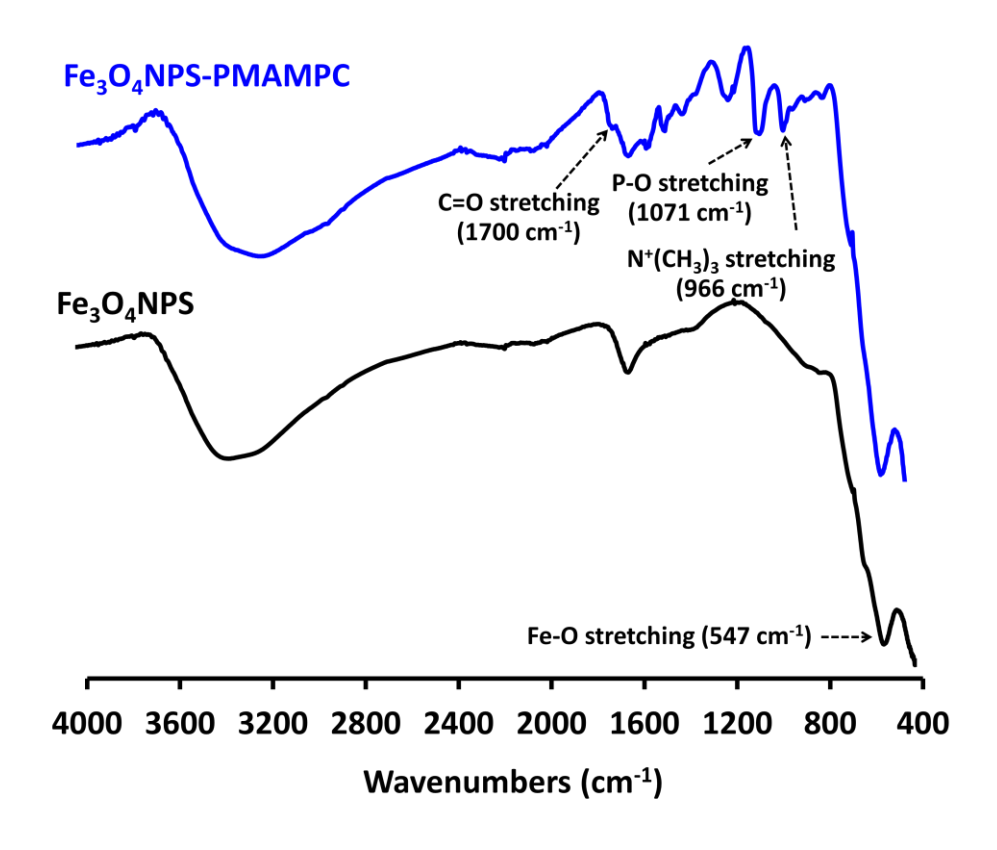


Figure 5. ATR-FTIR of uncoated Fe₃O₄NPs และ Fe₃O₄NPs-PMAMPC

The amount of PMAMPC coated on the Fe_3O_4NPs can be calculated from the weight loss as determined by TGA analysis. As seen in Figure 6, the uncoated Fe_3O_4NPs showed a major weight loss of 4% in a temperature range of 25-100 $^{\circ}C$ which should be due to loss of water. A similar magnitude of water loss from both types of PMAMPC- Fe_3O_4NPs was also found in the same temperature range. PMAMPC- Fe_3O_4NPs showed the additional weight loss between 200 and 400 $^{\circ}C$ which could be attributed to the thermal decomposition of the PMAMPC copolymer. The weight losses of 13.5 % corresponding to 9.7% of PMPC content were detected.

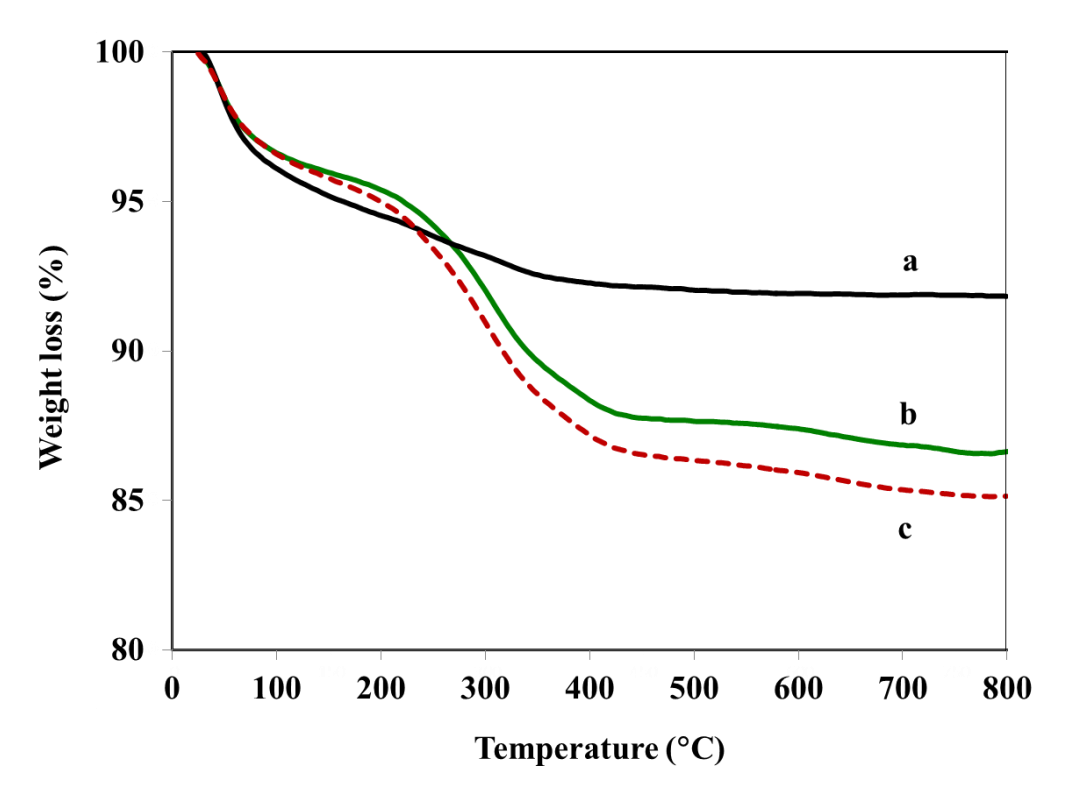


Figure 6. TGA curves of (a) uncoated Fe₃O₄NPs and (b) PMAMPC-Fe₃O₄NPs.

The TEM image shows that the PMAMPC-Fe₃O₄NPs are spherical and the average size is approximately 10.6 ± 1.3 nm (Figure 7). The stability of PMAMPC-Fe₃O₄NPs dispersion was determined by monitoring the settling of the nanoparticles in aqueous media. Black colloidal suspensions of PMAMPC-Fe₃O₄NPs showed good colloidal stability in aqueous media for up to 24 h of storage at room temperature (Figure 6). The PMAMPC-Fe₃O₄NPs could be rapidly separated from the dispersion using an external magnetic field for 5 min (Figure 8), showing they had an excellent magnetic response. The magnetization curves measured at room temperature for the PMAMPC-Fe₃O₄NPs are displayed in Figure 8. There was no residual magnetism or hysteresis loop in the magnetization, suggesting the Fe₃O₄NPs produced are superparamagnetic. High saturation magnetization values of 47 emu g⁻¹ were detected.

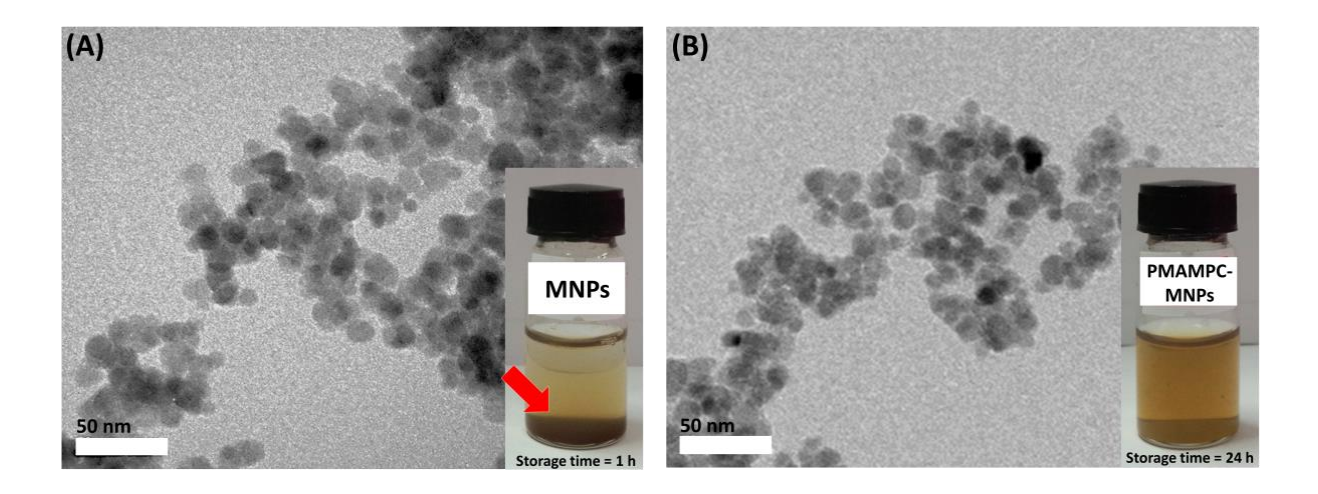
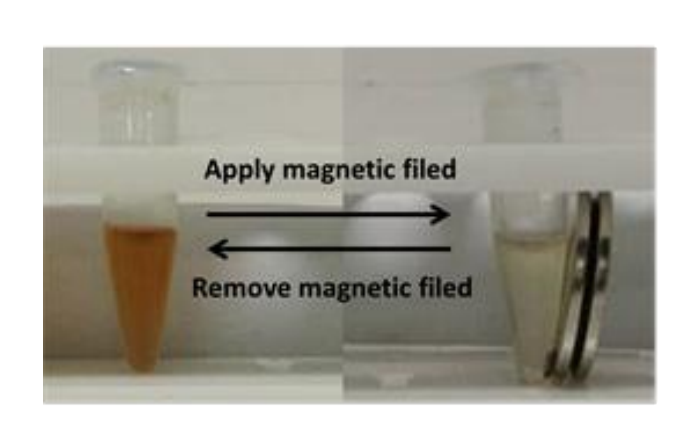


Figure 7. Pictures of uncoated Fe₃O₄NPs PMAMPC-e₃O₄NPs colloidal suspensions after 30-day of storage without an external magnetic field.



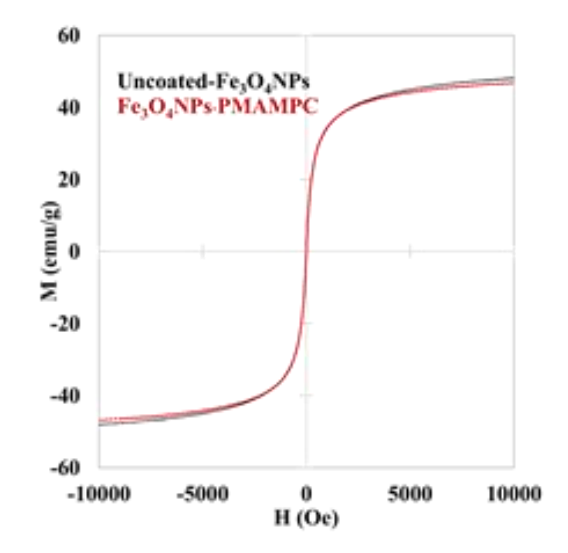


Figure 8. Pictures of PMAMPC- Fe_3O_4NPs colloidal after exposure to an external magnetic field (left) and magnetization curves of PMAMPC- Fe_3O_4NPs (right).

3.2 Immobilization of sensing probe

The immobilization of sensing probe (NH₂-aptamer) will be done via amide bond formation between the amino group of NH₂-aptamer and the carboxyl group of the MA unit in the PMAMPC coated on the surface of Fe₃O₄NPs via EDC/NHS coupling chemistry. As displayed in Figure 9, ATR-FTIR spectrum of the PMAMPC-Fe₃O₄NPs showed a characteristic C=O stretching of carboxyl groups at 1701 cm⁻¹. After aptamer conjugation, this peak disappeared while the new band at 1687 cm⁻¹ corresponded to an amide bond was observed, indicating that

the aptamers were successfully conjugated onto the surface of MNPs via a bond formation. The intensity of the new band at 1687 cm⁻¹ trended to increase with increasing the concentration of aptamer in feed.

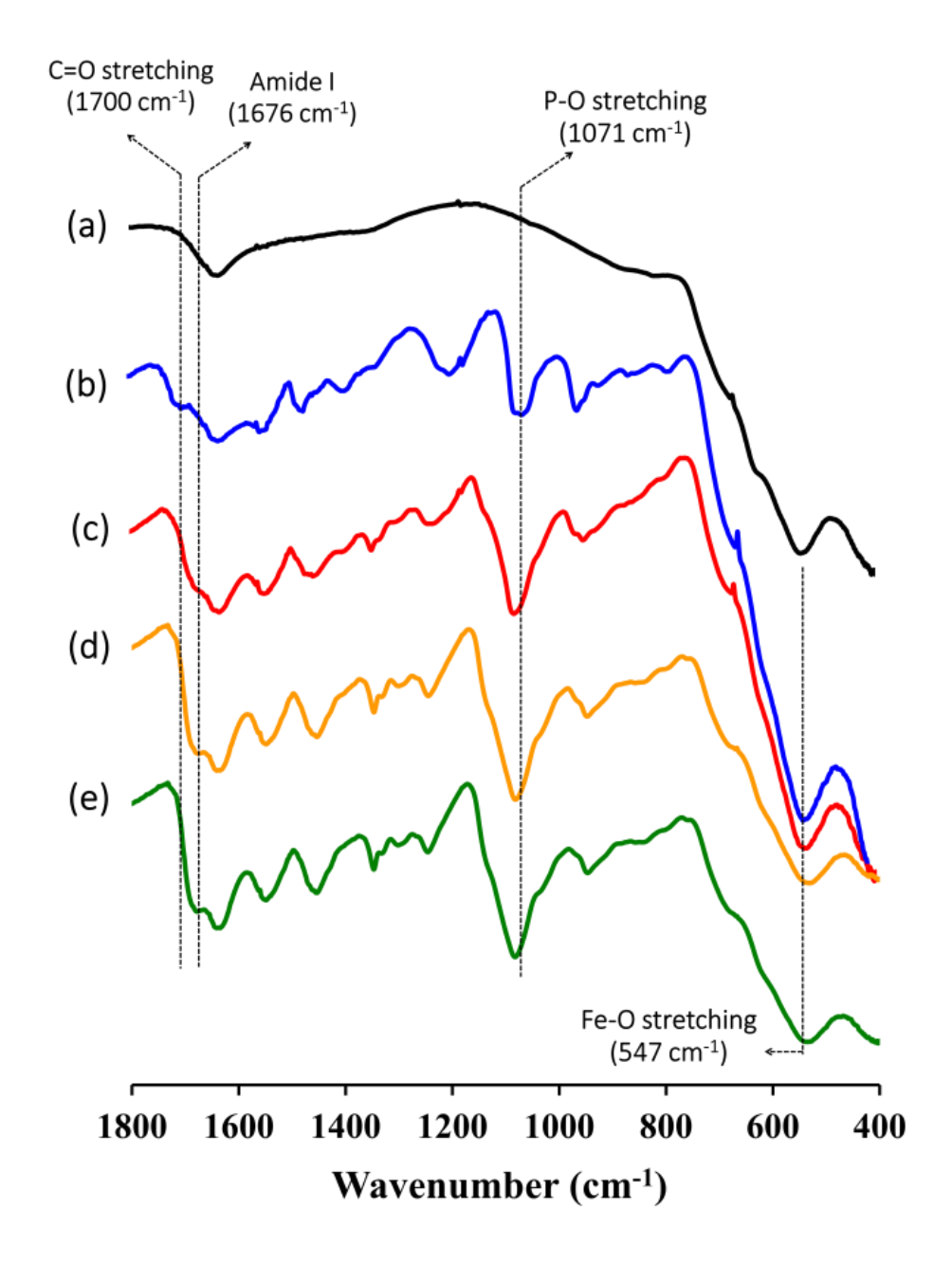


Figure 9. ATR-FTIR spectrum of uncoated Fe₃O₄NPs (a), Fe₃O₄NPs-PMAMPC (b), Apt-MNPs @12.5 μ L (c), Apt-MNPs @25 μ L (c) and Apt-MNPs @50 μ L (c).

The amounts of aptamer per nanoparticles in term of mass ratio, Q (mg/g) was calculated by an indirect method in which the concentration of the remaining FAM-labelled complementary DNA in the supernatant was measured and compared with the initial FAM-labelled complementary DNA by fluorescence spectrophotometer. The decrease of the fluorescence peak at 520 nm from initial FAM-labelled complementary DNA (Figure 10a) to remaining FAM-labelled complementary DNA (Figure 10b, c and d) was observed upon aptamer conjugation (Figure 10). The effect of the aptamer concentration on

the conjugation efficiency was demonstrated. The decrease of the fluorescence peak increased with increasing aptamer concentration. The Q value was 1.45 mg/g, 2.59 mg/g and 3.28 for aptamer concentration at 12.5, 25 and 50 μ M, respectively.

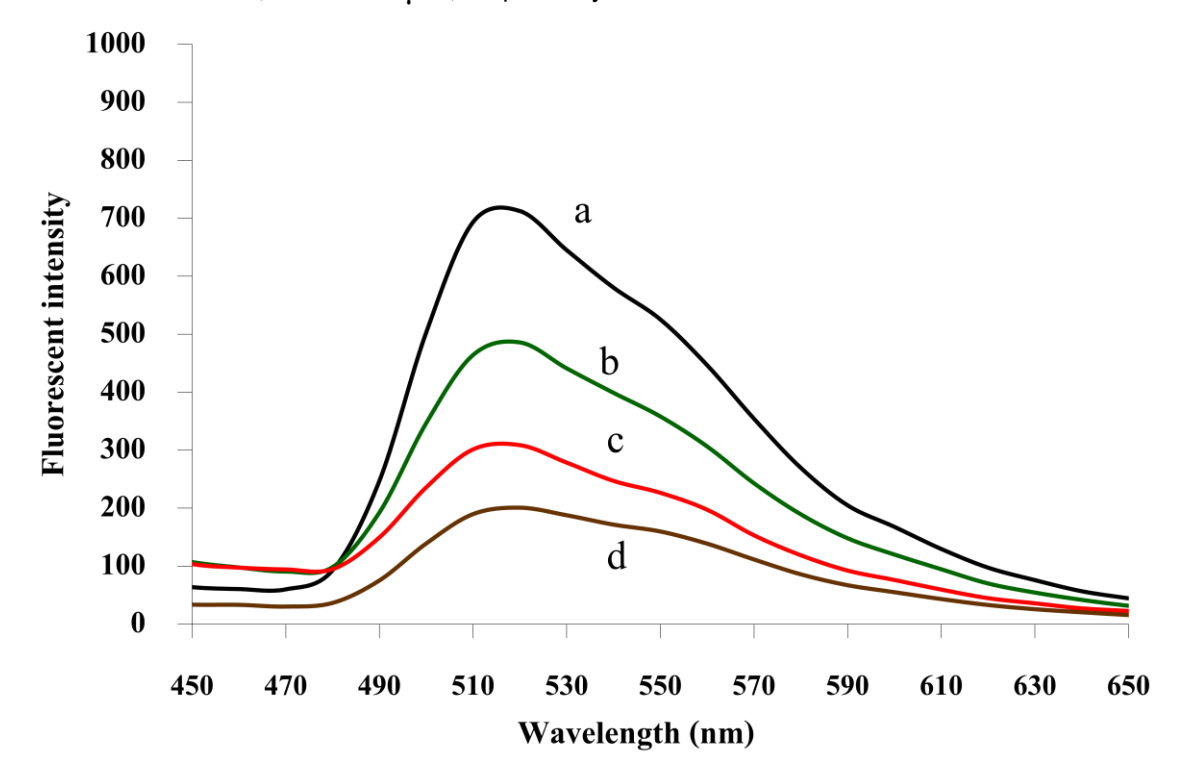


Figure 10. Fluorescence spectra of initial FAM-labelled complementary DNA (a), remaining FAM-labelled complementary DNA@12.5 μ M apt (b), remaining FAM-labelled complementary DNA@25 μ M apt, and remaining FAM-labelled complementary DNA@50 μ M apt.

3.3 Investigation of peroxidase catalytic activity

Naturally, the magnetite nanoparticles can catalyze the oxidation of peroxidase substrate such as TMB in the presence of H_2O_2 , and subsequently a blue colour product, an oxidized form TMB. The time dependent catalytic activity of uncoated Fe_3O_4NPs , Fe_3O_4NPs -PMAMPC and Apt-MNPs was displayed in Figure 11. The catalytic activity of Fe_3O_4NPs -PMAMPC and Apt-MNPs slightly decreased after functionalization. The different amount of aptamer immobilization was not affected to the catalytic activity (Figure 12).

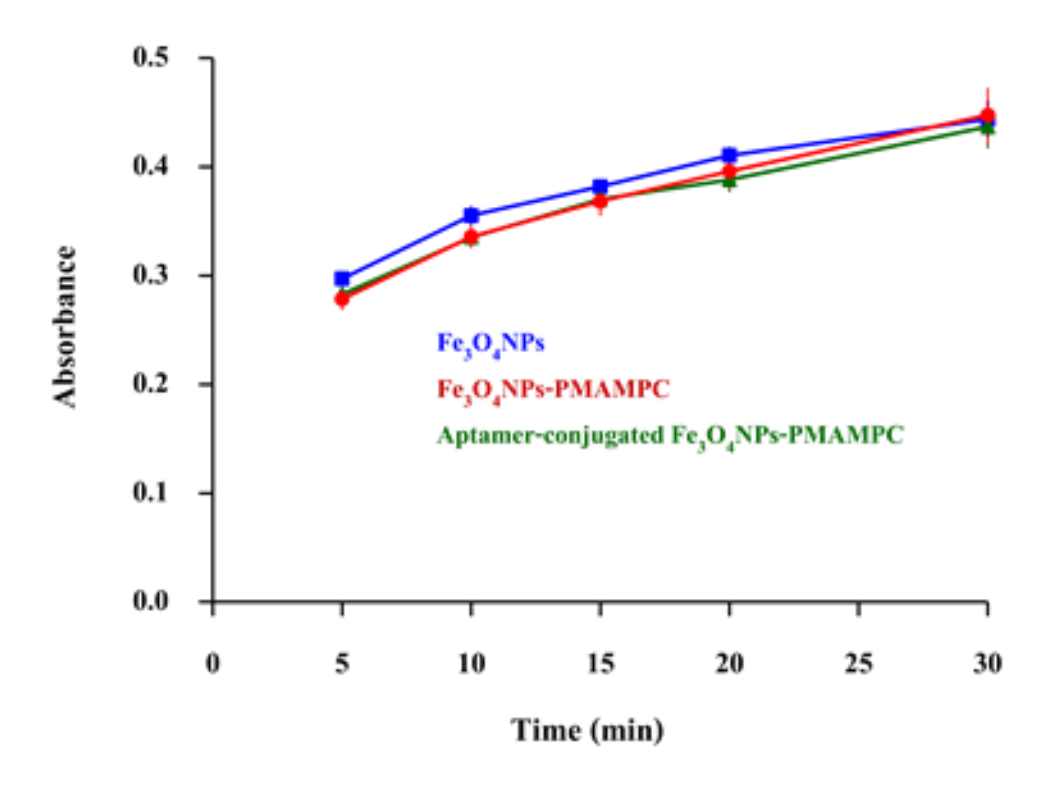


Figure 11. The catalytic activity of uncoated Fe₃O₄NPs, Fe₃O₄NPs-PMAMPC and Apt-MNPs

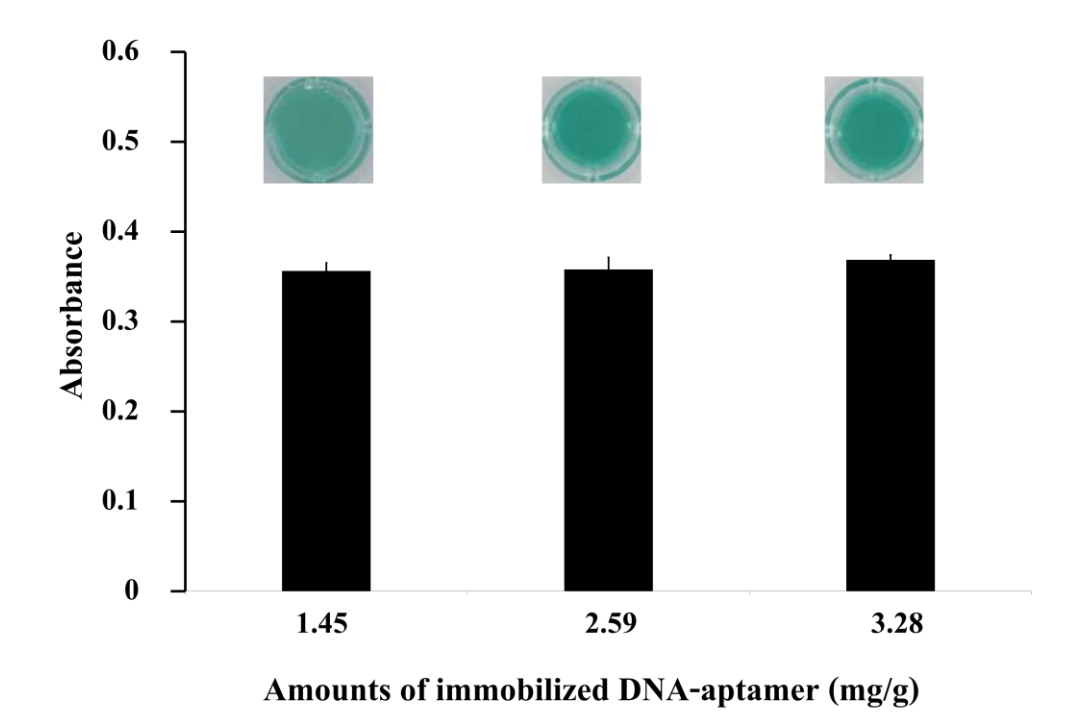


Figure 12. The catalytic activity of Apt-MNPs at different amount of aptamer immobilization

3.4 Examination of colorimetric assay for bacteria detection

One-step detection mechanism is designed based on the concept of target-induced shielding effect whereby the peroxidase-like behavior of aptamer-conjugated Fe₃O₄NPs would be suppressed in the presence of bacteria (Figure 13). The binding between aptamer located on the surface of Fe₃O₄NPs and bacteria would induce the aggregation of multiple Fe₃O₄NPs, causing the inhibition of Fe₃O₄NPs to catalyze the oxidation of TMB in the presence of H₂O₂. Therefore, the colorimetric signal off depended on the presence of target bacteria while the colorimetric signal on was maximal in the absence of the target. In this concept, the detection of bacteria could be read out by the naked eye and UV-visible spectrophotometer.

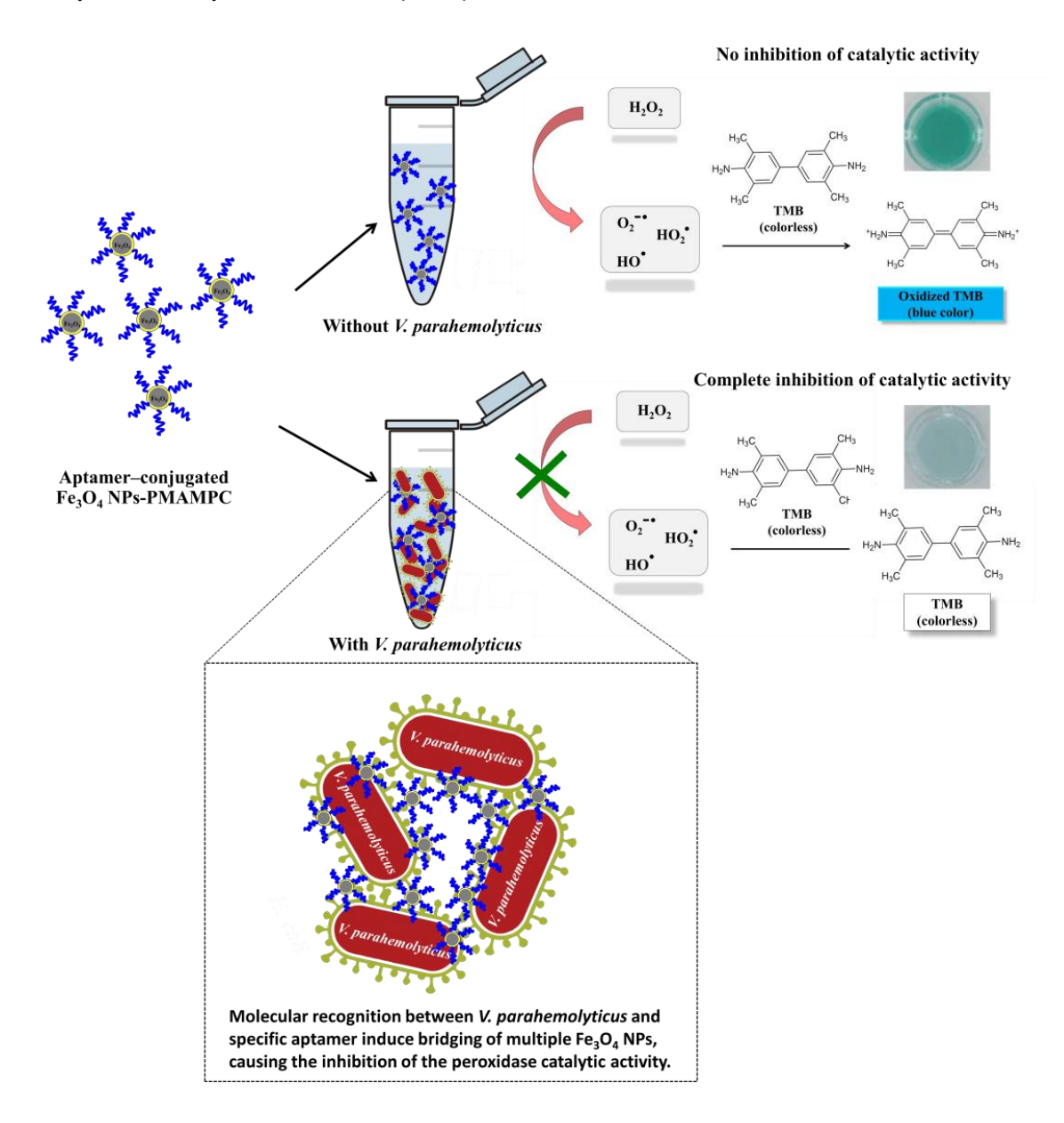


Figure 13. Schematic representation of colorimetric detection of a foodborne pathogen by aptamer-conjugated Fe₃O₄NPs.

To demonstrate the utility of this proposed methodological approach, we used aptamer-conjugated Fe_3O_4NPs having DNA aptamer against V. parahaemolyticus. Figure 14 shows that the colorimetric signal of aptamer-conjugated Fe_3O_4NPs in the presence of V. parahaemolyticus was significantly reduced in comparison with the signal coming from the absence of V. parahaemolyticus. Importantly, in case of non-aptamer conjugated Fe_3O_4NPs , the colorimetric signal was slightly decreased after incubation with V. parahaemolyticus. This result clearly showed that the decrease of colorimetric signal would enhance by the specific binding between aptamer located on the Fe_3O_4NP and V. parahaemolyticus.

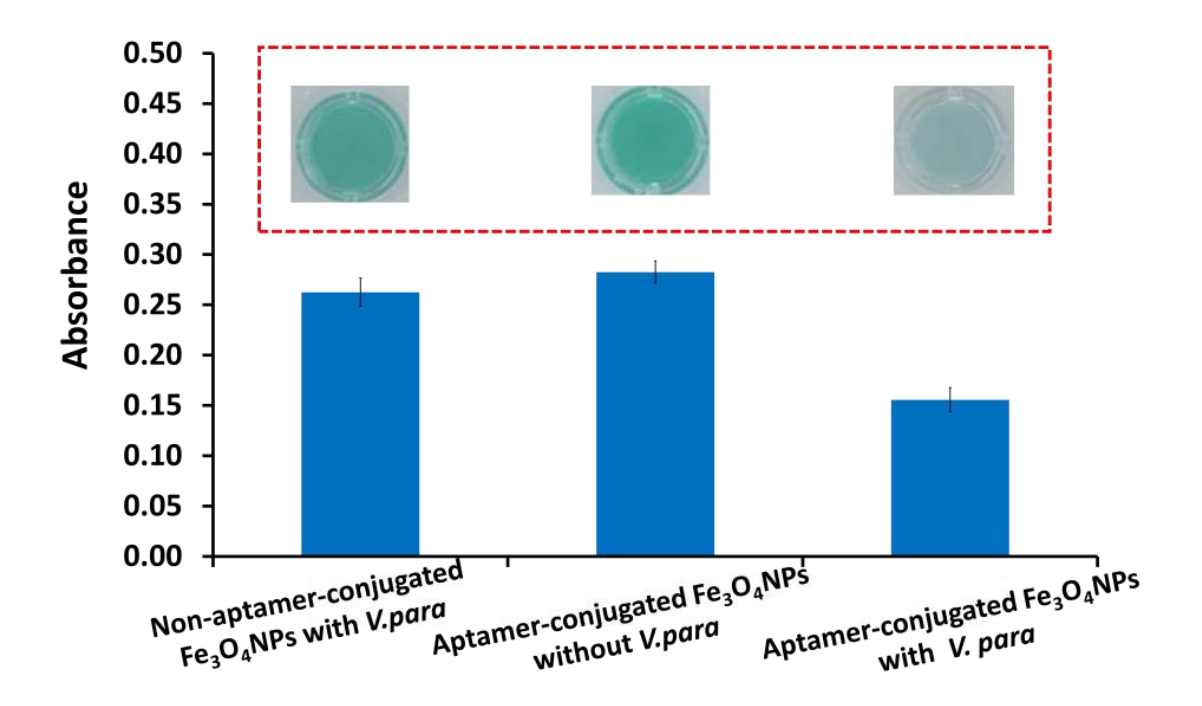
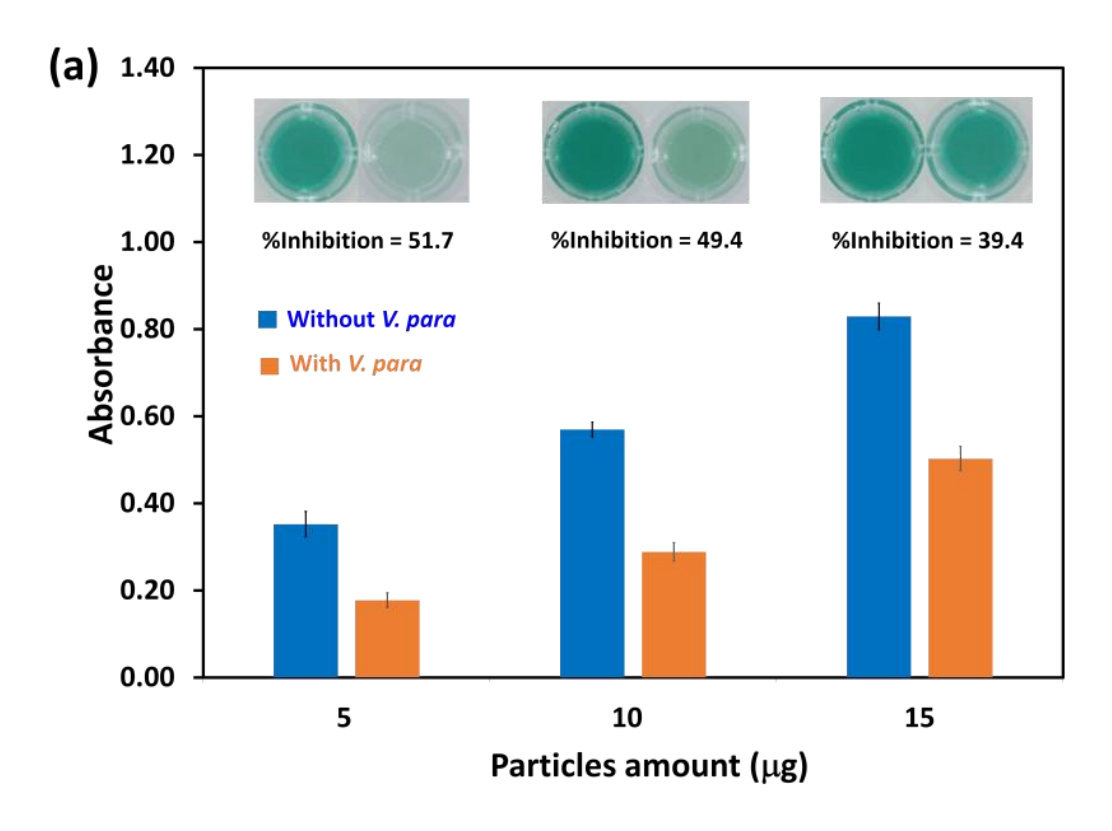


Figure 14. Schematic representation of colorimetric detection of V. parahaemolyticus by aptamer-conjugated Fe_3O_4NPs

In order to get the maximal colorimetric signal, we optimized experimental conditions for colorimetric detection of the *V. parahaemolyticus*. The amount of the nanoparticles and the conjugated aptamer are important factor that influence on the detection efficiency. Therefore, different amount of the nanoparticles were applied to detect the *V. parahaemolyticus*. As shown in Figure 15, the change in catalytic activity of the nanoparticles was observed where *V. parahaemolyticus* was added to aptamer-conjugated Fe_3O_4NPs . However, the maximal colorimetric signal in term of % inhibition was observed when the 5 μ g of the nanoparticles were used. The highest amount of conjugated aptamer (32.8 mg/g) provided the maximal colorimetric signal with 60.4% of inhibition value. The result might be attributed that higher content of aptamer on the surface of Fe_3O_4NPs provide a greater possibility of aptamer to bind with *V. parahaemolyticus*. Consequently, the ability of aptamer-conjugated Fe_3O_4NPs to catalyze the oxidation of TMB is prohibited. We also optimized the catalytic reaction, e.g., by varying H_2O_2 and TMB concentrations. With the optimized conditions of 20 μ L H_2O_2 and 20 μ L TMB, the colorimetric signal of the sample having *V. parahaemolyticus* was significantly reduced (Figure 16).



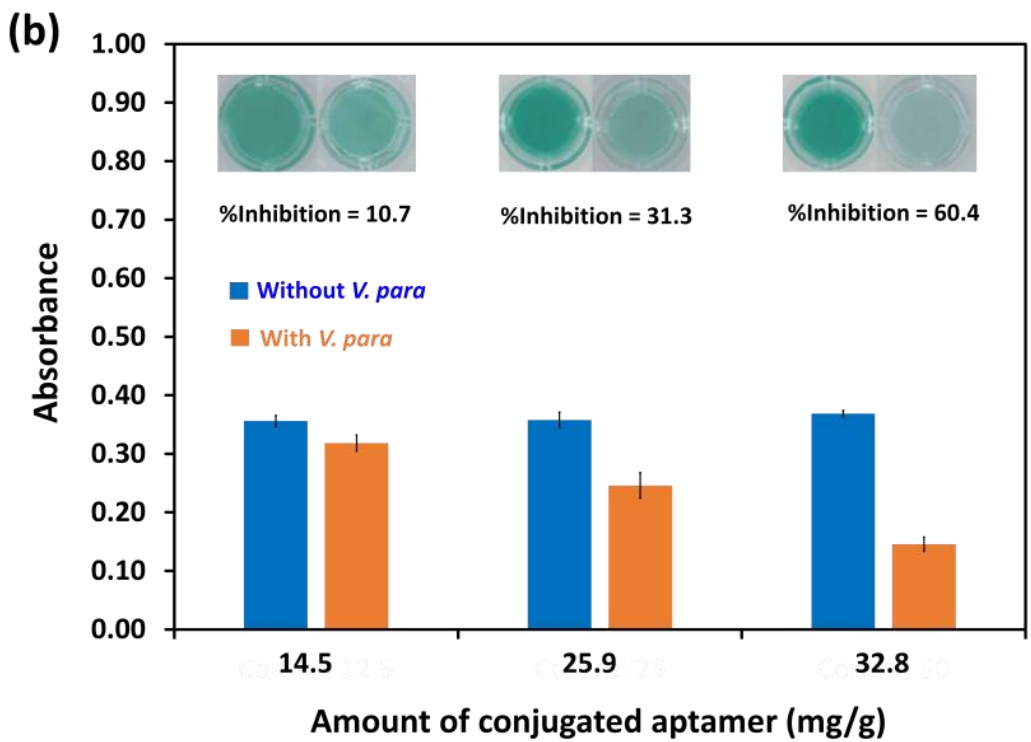


Figure 15. Optimization of the nanoparticles amount (A) and the conjugated aptamer amount (B). The concentration of *V. parahemolyticus* was 10⁴ cfu/mL.

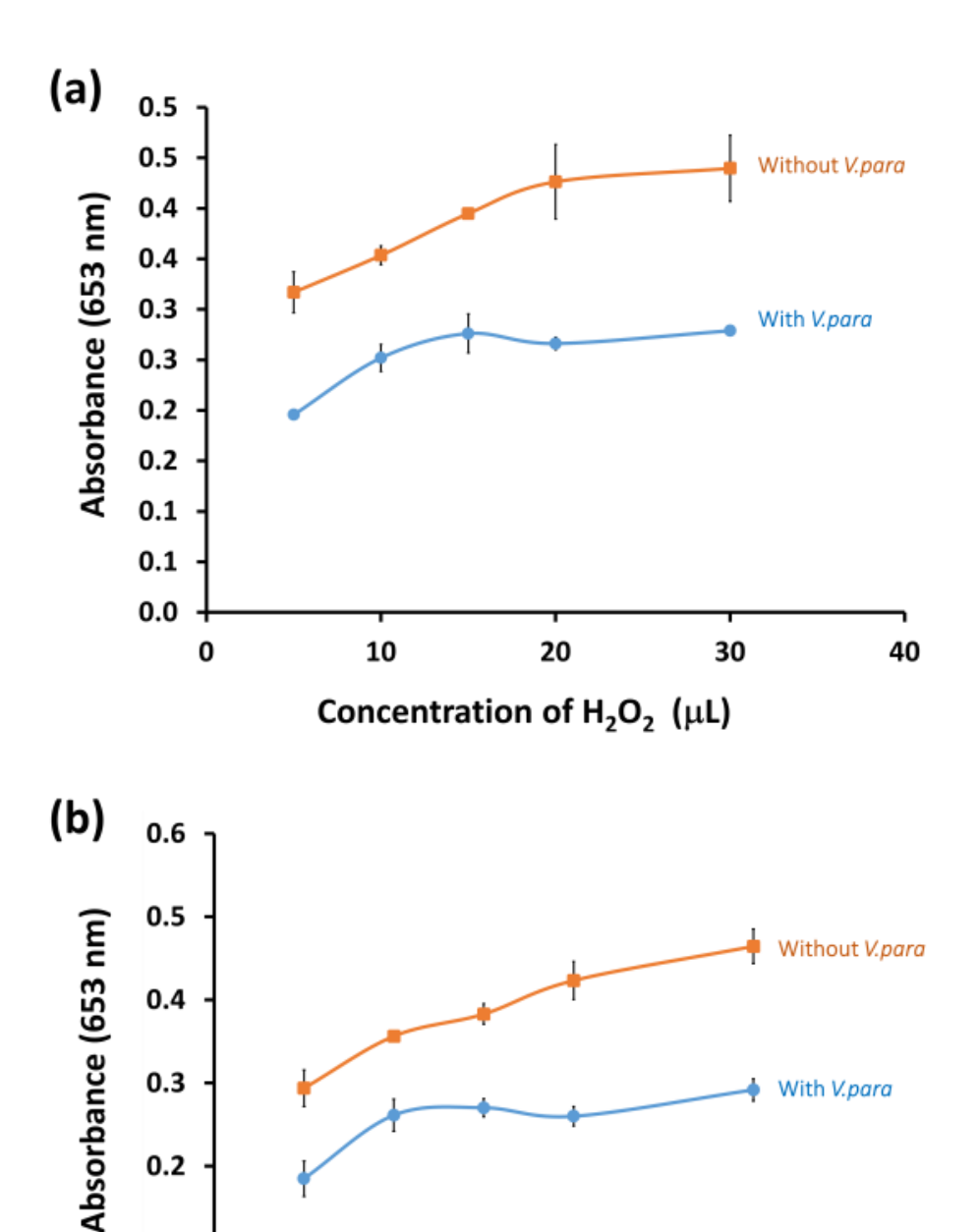


Figure 16. Optimization of H_2O_2 concentration (A) and TMB concentration (B). The concentration of V. parahemolyticus was 104 cfu/mL.

20

Concentration of TMB (µL)

3.4.1 Detection of *V. parahaemolyticus* in the pure cultures

10

0.3

0.2

0.1

0

0

In principle, the catalytic activity would drastically reduce in proportion to the V. parahaemolyticus concentration. The results in Figure 17a presented the decreasing of blue color when the concentration of V. parahaemolyticus increased from 101 to 105 CFU/mL. The difference in the color between the 101 CFU/mL of V. parahaemolyticus and the blank control was clearly identified by naked eyes. From the corresponding absorption

With V.para

40

30

data shown in Figure 17b, there was a good negative linear relationship between the absorbance and the concentration of V. parahaemolyticus in the range of 10^1 to 10^5 CFU/mL, with the linear equation of y=-0.0476x+0.3961 ($R^2=0.9708$) displayed in Figure 5c. The limit of detection (LOD) defined as the lowest concentration of bacteria that give a signal three times higher than the standard deviation of blank was calculated by LOD = 3SDblank /slope. Thus the LOD for V. parahaemolyticus in the pure cultures was 3 CFU/mL.

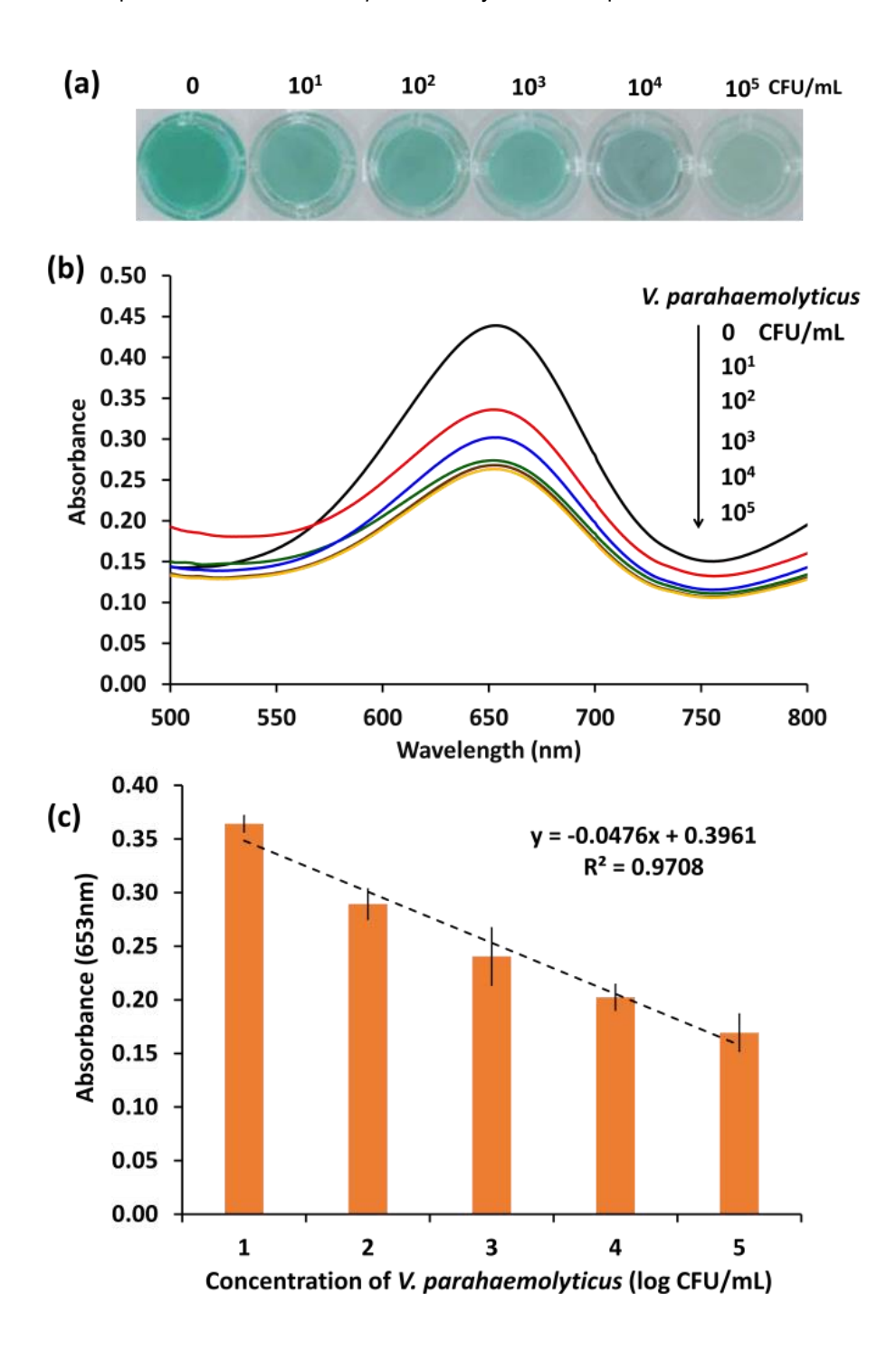
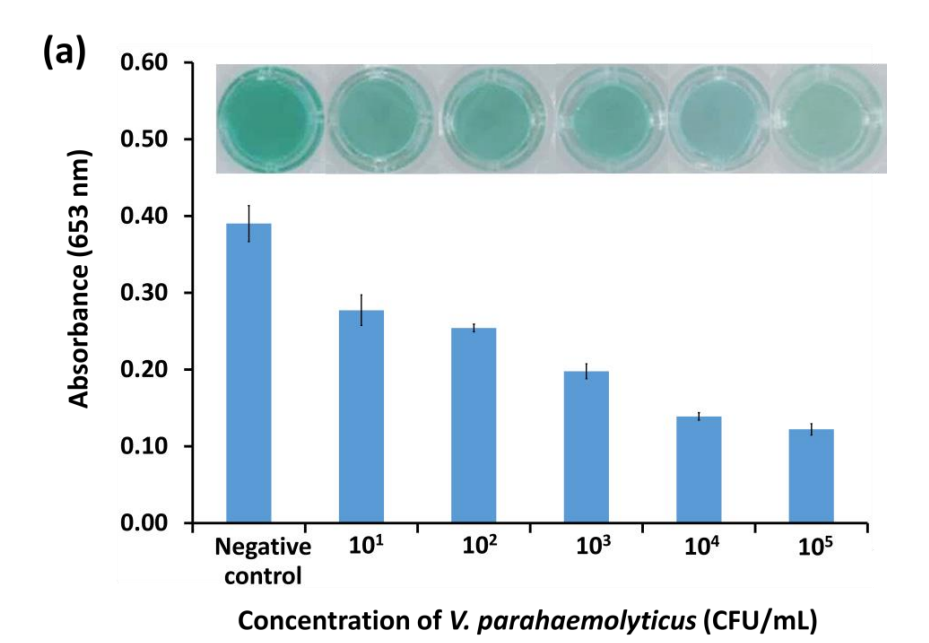


Figure 17. (A) Optical images and (B) absorption spectra form the detection of different concentrations of *V. parahaemolyticus*. (C) Standard curve of the related absorbance versus the log concentration of *V. parahaemolyticus*.

3.4.2 Detection of V. parahaemolyticus in spiked samples

The applicability of this proposed method was further tested in spiked oyster samples. The different concentrations of the *V. parahaemolyticus* were added to oyster samples. Then, the spiked samples were analyzed by the developed method. As can be seen from Figure 18a, the blue color decresed when *V. parahaemolyticus* presented in samples. Moerover, the decrease of blue color increased with increasing the concentration of *V. parahaemolyticus* from 10 to 10⁵ CFU/mL. From the corresponding absorption data shown in Figure 18b, there was a good negative linear relationship between the absorbance and the concentration of *V. parahaemolyticus* as in case of the pure cultures.



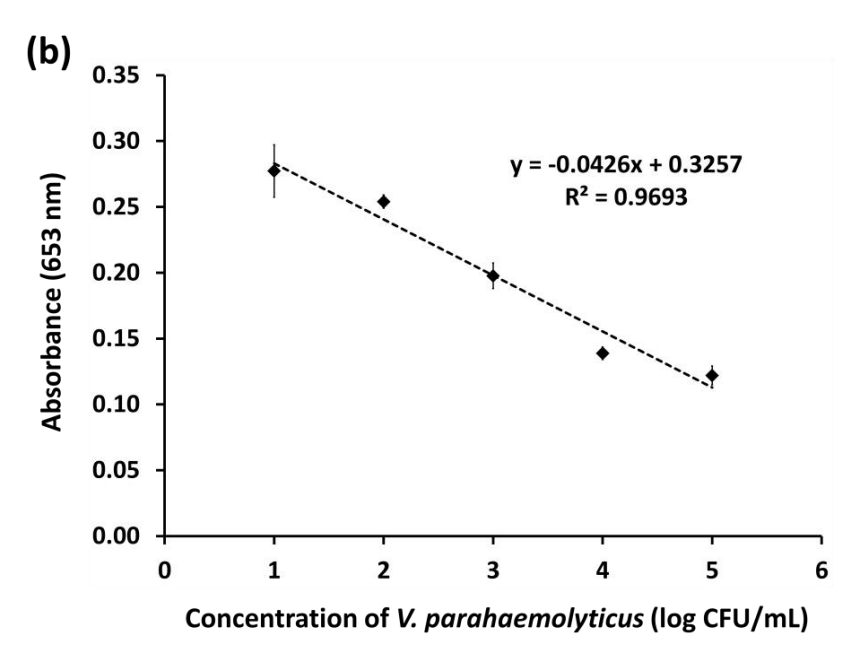


Figure 18. (A) Absorption spectra and relevance optical images form the detection of *different concentrations* of *V. parahaemolyticus* in spiked samples. (B) Standard curve of the related absorbance versus the log concentration of *V. parahaemolyticus*.

To investigate the selectivity of developed method the aptamer-conjugated Fe₃O₄NPs were employed to detect other pathogenic bacteria at a concentration of 10⁴ cfu/mL. As shown in Figure 19, it is clearly seen that only *V. parahaemolyticus* induces a dramatic decrease of signal response, whereas other species produced signals as high as the negative control (in the absence of *V. parahaemolyticus*). These results clearly demonstrated that the developed method specifically identified of *V. parahaemolyticus*.

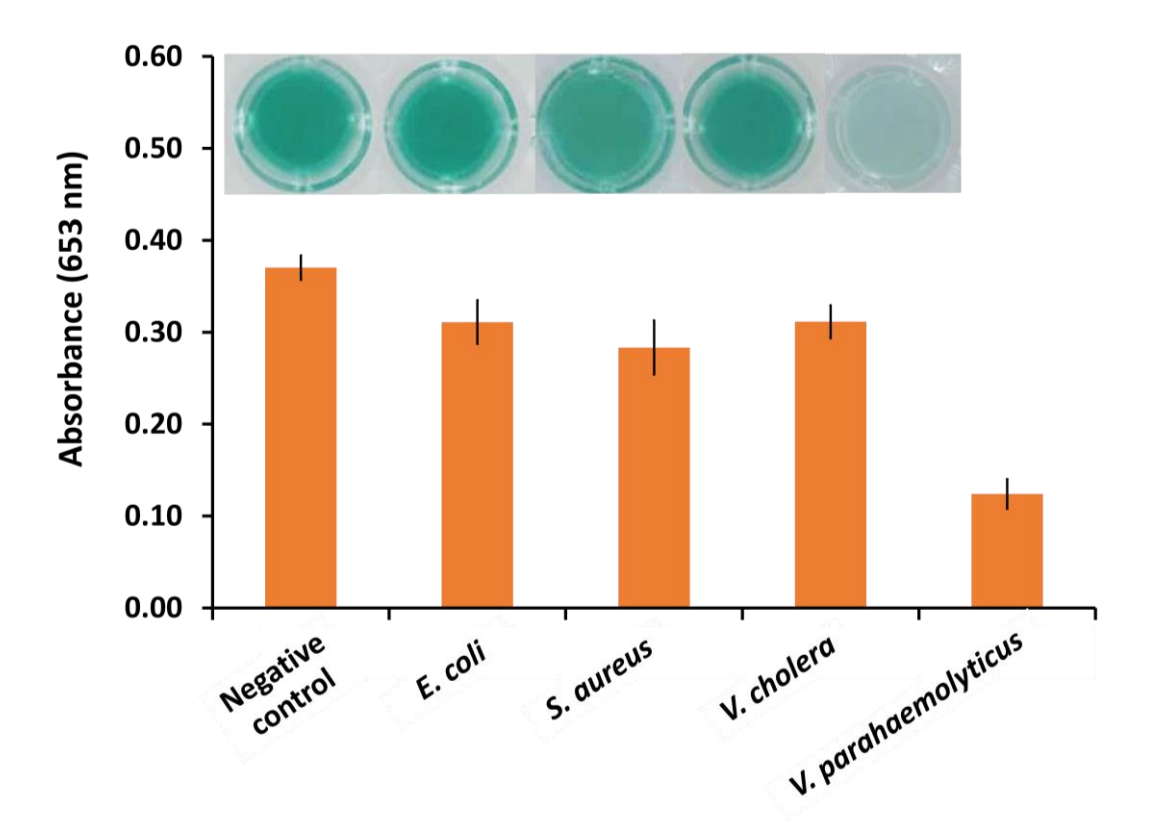


Figure 19. Specificity evaluation against other bacteria. Concentration of bacteria was 10⁴ cfu/mL

4. CONCLUSION

A simple colorimetric assay for *V. parahaemolyticus* detection based on enzyme-mimic catalytic activity of aptamer-conjugated Fe₃O₄NPs-PMAMPC has been successfully developed. One-step detection mechanism was designed based on the concept of target-induced shielding effect whereby the catalytic activity of aptamer-conjugated Fe₃O₄NPs-PMAMPC would be suppressed in the presence of bacteria. The decrease of color change could be realized by naked eye. The specific capture between aptamer and target bacteria is the key to success. By employing the specific *V. parahaemolyticus* aptamer as a bacterial specific recognition element, this assay displayed excellent specificity. This assay has the potential to be detected *V. parahaemolyticus* in oyster samples. It should be highlighted that this assay does not require additional step for signal amplification as traditional assay, ELISA or PCR technology.

5. REFERENCE

- Akkahat, P., Kiatkamjornwong, S., Yusa, S. I., Hoven, V. P., & Iwasaki, Y. (2012) Development of a novel antifouling platform for biosensing probe immobilization from methacryloyloxyethyl phosphorylcholine-containing copolymer brushes. *Langmuir*, 28(13), 5872-5881.
- Andrade, A.L., Souza, D.M., Pereira, M.C., Fabris, J. D., & Domingues, R.Z. (2009). Magnetic properties of nanoparticles obtained by different chemical routes. *Journal of Nanoscience and Nanotechnology*, 9(3), 2081-2087.
- Chen, Y., Xianyu, Y., Wang, Y., Zhang, X., Cha, R., Sun, J., & Jiang, X. (2015). One-step detection of pathogens and viruses: combining magnetic relaxation switching and magnetic separation. ACS nano, 9(3), 3184-3191.
- 4. Cheng, K., Pan, D., Teng, J., Yao, L., Ye, Y., Xue, F., ... & Chen, W. (2016). Colorimetric integrated pCR protocol for rapid detection of Vibrio parahaemolyticus. *Sensors*, 16(10), 1600.
- Chiu, Y. C., & Chen, Y. C. (2008). Carboxylate Functionalized Iron Oxide Nanoparticles in Surface Assisted Laser Desorption/Ionization Mass Spectrometry for the Analysis of Small Biomolecules. *Analytical Letters*, 41(2), 260-267.
- Cirtiu, C. M., Raychoudhury, T., Ghoshal, S., & Moores, A. (2011). Systematic comparison of the size, surface characteristics and colloidal stability of zero valent iron nanoparticles pre-and post-grafted with common polymers. *Colloids and Surfaces A: Physicochemical and Engineering Aspects*, 390(1), 95-104.
- 7. Di Pinto, A., Terio, V., Di Pinto, P., Colao, V., & Tantillo, G. (2012). Detection of Vibrio parahaemolyticus in shellfish using polymerase chain reaction—enzyme linked immunosorbent assay. Letters in applied microbiology, 54(6), 494-498.
- 8. Gao, L., Zhuang, J., Nie, L., Zhang, J., Zhang, Y., Gu, N., ... & Yan, X. (2007). Intrinsic peroxidase-like activity of ferromagnetic nanoparticles. *Nature nanotechnology*, 2(9), 577-583.
- 9. Huang, J., Wan, S., Guo, M., & Yan, H. (2006). Preparation of narrow or mono-disperse crosslinked poly(meth)acrylic acid)/iron oxide magnetic microspheres. *Journal of Materials Chemistry*, 16(1), 4535-4541
- 10. Hyeon, J. Y., & Deng, X. (2017). Rapid detection of Salmonella in raw chicken breast using real-time PCR combined with immunomagnetic separation and whole genome amplification. *Food microbiology*, 63, 111-116.
- 11. Jiang, H., Han, X., Li, Z., Chen, X., Hou, Y., Gai, L., ... & Fu, T. (2012). Superparamagnetic coreshell structured microspheres carrying carboxyl groups as adsorbents for purification of genomic DNA. *Colloids and Surfaces A: Physicochemical and Engineering Aspects*, 401, 74-80.
- 12. Kim, S. H., Lee, Y. S., & Kwak, H. S. (2016). Rapid real-time PCR for the detection of Vibrio parahaemolyticus in seafood. *International Journal of Infectious Diseases*, 53, 69.
- 13. Kumar, B. K., Raghunath, P., Devegowda, D., Deekshit, V. K., Venugopal, M. N., Karunasagar, I., & Karunasagar, I. (2011). Development of monoclonal antibody based sandwich ELISA for the rapid

- detection of pathogenic Vibrio parahaemolyticus in seafood. *International journal of food microbiology*, 145(1), 244-249.
- 14. Li, X., Wen, F., Creran, B., Jeong, Y., Zhang, X., & Rotello, V. M. (2012). Colorimetric protein sensing using catalytically amplified sensor arrays. Small, 8(23), 3589-3592.
- 15. Liu, Q., Li, H., Zhao, Q., Zhu, R., Yang, Y., Jia, Q., Bian, B., & Zhuo, L. (2014). Glucose-sensitive colorimetric sensor based on peroxidase mimics activity of porphyrin-Fe₃O₄ nanocomposites. *Materials Science and Engineering C*, 41, 142–151.
- 16. Liu, X.Y., Zheng, S. W., Hong, R. Y., Wang, Y. Q., & Feng, W. G. (2014). Preparation of magnetic poly(styrene-co-acrylic acid) microspheres with adsorption of protein. *Colloids and Surfaces A: Physicochemical and Engineering Aspects*, 443, 425–431.
- 17. Lu, W., Shen, Y., Xie, A., & Zhang, W. (2013). Preparation and drug-loading properties of Fe₃O₄/Poly (styrene-co-acrylic acid) magnetic polymer nanocomposites. *Journal of Magnetism and Magnetic Materials*, 345, 142–146
- 18. Mahmoudi, M., Sant, S., Wang, B., Laurent, S., & Sen, T. (2011). Superparamagnetic iron oxide nanoparticles (SPIONs): development, surface modification and applications in chemotherapy. *Advanced drug delivery reviews*, 63(1), 24-46.
- Mao, Y., Huang, X., Xiong, S., Xu, H., Aguilar, Z. P., & Xiong, Y. (2016). Large-volume immunomagnetic separation combined with multiplex PCR assay for simultaneous detection of Listeria monocytogenes and Listeria ivanovii in lettuce. *Food Control*, 59, 601-608.
- 20. Nishizawa, K., Takai, M., & Ishihara, K. (2011). A bioconjugated phospholipid polymer biointerface with nanometer-scaled structure for highly sensitive immunoassays. *Bioconjugation Protocols:* Strategies and Methods, 491-502.
- 21. Park, J., Kurosawa, S., Takai, M., & Ishihara, K. (2007). Antibody immobilization to phospholipid polymer layer on gold substrate of quartz crystal microbalance immunosensor. *Colloids and Surfaces B: Biointerfaces*, 55(2), 164-172.
- 22. Park, K. S., Kim, M. I., & Park, H. G. (2011). Label-Free colorimetric detection of nucleic acids based on target-induced shielding against the peroxidase-mimicking activity of magnetic nanoparticles. *Small*, 7(11), 1521–1525.
- 23. Shukla, S., Lee, G., Song, X., Park, S., & Kim, M. (2016). Immunoliposome-based immunomagnetic concentration and separation assay for rapid detection of Cronobacter sakazakii. *Biosensors and Bioelectronics*, 77, 986-994.
- 24. Tajima, N., Takai, M., & Ishihara, K. (2011). Significance of antibody orientation unraveled: well-oriented antibodies recorded high binding affinity. *Analytical chemistry*, 83(6), 1969-1976.
- 25. Wan, Y., Sun, Y., Qi, P., Wang, P., & Zhang, D. (2014). Quaternized magnetic nanoparticles—fluorescent polymer system for detection and identification of bacteria. *Biosensors and Bioelectronics*, 55, 289-293.
- 26. Wang, G., Zhang, X., Skallberg, A., Liu, Y., Hu, Z., Mei, X., & Uvdal, K. (2014). One-step synthesis of water-dispersible ultra-small Fe 3 O 4 nanoparticles as contrast agents for T 1 and T 2 magnetic resonance imaging. *Nanoscale*, 6(5), 2953-2963.

- Ward, L. N., & Bej, A. K. (2006). Detection of Vibrio parahaemolyticus in shellfish by use of multiplexed real-time PCR with TaqMan fluorescent probes. *Applied and environmental microbiology*, 72(3), 2031-2042.
- 28. Woo, M. A., Kim, M. I., Jung, J. H., Park, K. S., Seo, T. S., & Park, H. G. (2013). A novel colorimetric immunoassay utilizing the peroxidase mimicking activity of magnetic nanoparticles. *International journal of molecular sciences*, 14(5), 9999-10014.
- 29. Xu, Y., Zhuang, L., Lin, H., Shen, H., & Li, J. W. (2013). Preparation and characterization of polyacrylic acid coated magnetite nanoparticles functionalized with amino acids. *Thin Solid Films*, 544, 368-373.
- 30. Yamazaki, W., Kumeda, Y., Misawa, N., Nakaguchi, Y., & Nishibuchi, M. (2010). Development of a loop-mediated isothermal amplification assay for sensitive and rapid detection of the tdh and trh genes of Vibrio parahaemolyticus and related Vibrio species. *Applied and environmental microbiology*, 76(3), 820-828.
- 31. Zeng, J., Wei, H., Zhang, L., Liu, X., Zhang, H., Cheng, J., ... & Liu, L. (2014). Rapid detection of Vibrio parahaemolyticus in raw oysters using immunomagnetic separation combined with loop-mediated isothermal amplification. *International journal of food microbiology*, 174, 123-128.
- 32. Zhang, Z., Wang, Z., Wang, X., & Yang, X. (2010). Magnetic nanoparticle-linked colorimetric aptasensor for the detection of thrombin. *Sensors and Actuators B: Chemical*, 147(2), 428-433.
- 33. Zhu, R. G., Li, T. P., Jia, Y. F., & Song, L. F. (2012). Quantitative study of viable Vibrio parahaemolyticus cells in raw seafood using propidium monoazide in combination with quantitative PCR. *Journal of microbiological methods*, 90(3), 262-266.